

# Coherent Oscillations: A Mechanism of Feature Linking in the Visual Cortex?

## Multiple Electrode and Correlation Analyses in the Cat

R. Eckhorn, R. Bauer, W. Jordan, M. Brosch, W. Kruse, M. Munk, and H. J. Reitboeck

Fachbereich Physik, Angewandte Physik und Biophysik, Philipps-Universität, Renthof 7, D-3550 Marburg, Federal Republic of Germany

**Abstract.** *Primary visual coding* can be characterized by the receptive field (RF) properties of single neurons. Subject of this paper is our search for a global, *second coding step* beyond the RF-concept that links related features in a visual scene. In recent models of visual coding, oscillatory activities have been proposed to constitute such linking signals. We tested the neurophysiological relevance of this hypothesis for the visual system. Single and multiple spikes as well as local field potentials were recorded simultaneously from several locations in the primary visual cortex (A17 and A18) using 7 or 19 individually advanceable fiber-microelectrodes (250 or 330  $\mu\text{m}$  apart). *Stimulus-evoked (SE)-resonances* of 35–85 Hz were found in these three types of signals throughout the visual cortex when the primary coding channels were activated by their specific stimuli. Stimulus position, orientation, movement direction and velocity, ocularity and stationary flicker caused specific SE-resonances. *Coherent SE-resonances* were found at distant cortical positions when at least one of the primary coding properties was similar. Coherence was found 1) within a vertical cortex column, 2) between neighbouring hypercolumns, and 3) between two different cortical areas. We assume that the coherence of SE-resonances is mediated by recurrent excitatory intra- and inter-areal connections via phase locking between assemblies that represent the linking features of the actual visual scene. Visually related activities are, thus, transiently labelled by a temporal code that signalizes their momentary association.

subsequent processing operations. It is still largely unknown how the visual system links features of a visual scene that belong together. We have proposed that a possible and efficient mechanism for the linking of regions and attributes that define the pattern could be based on temporal signal correlations, and that the partial coherence of action potentials within a neural population could be an operating principle for pattern definition and for the correlation of pattern attributes (Reitboeck 1983b). We also developed a model of texture definition based on temporal signal parameters. The basic concept of the model is that eye movements do convert spatial texture intervals into temporal spike intervals. Temporal gating of those signals can thus generate texture region separation (Reitboeck et al. 1987). A shortcoming of our model in its first definition was its rigid stimulus-response coupling. It must be possible, however, that control signals from higher processing stages can override the stimulus-induced linking in order to connect regions according to higher interpretation criteria based on structure, context, function etc. The initial neural response, therefore, should still be flexible and undefined in at least one parameter. The stimulus-evoked (SE)-resonances described in this paper would perfectly fulfill this requirement.

In this neurophysiological study we were mainly interested in mechanisms of pre-attentive *feature linking* at primary coding channels that are defined by the receptive field (RF) properties of single cells. At this processing stage, *linking features* can be: *proximity in visual space* (see the concept of local sign (Koenderink 1984)), *local similarities of spatial frequency and texture* (e.g. Reichardt 1957; Reichardt et al. 1983; Reitboeck et al. 1987, 1988) or *similarity of movement directions and velocities*. *Near-simultaneity of events* is also a linking feature (e.g. Wilson and Singer 1981; Altmann et al. 1986; von der Malsburg 1983; Reitboeck et al. 1987; Eckhorn et al. 1988a–c).

---

## 1 Introduction

A basic requirement in any pattern recognition task is object separation. Object regions must be labelled and linked so that objects can be treated as entities in

Several models have been proposed in which correlated activities play a prominent role for global sensory coding. In this paper, models that include oscillatory activities are of primary interest (Grossberg 1976, 1980; Başar 1983; Reitboeck 1983b, 1988; von der Malsburg 1983; Johannesma et al. 1986; von der Malsburg and Schneider 1986; Reitboeck et al. 1987, 1988; Eckhorn et al. 1988a–c). Based on our experimental results, we propose that visual features having a high degree of “relatedness” do evoke coherent SE-resonances and that these correlations act as temporal labels that link features into a perceptual entity.

*Experimentally*, questions of global dynamic coding can be studied with simultaneous multiple site recordings (e.g. Reitboeck 1983a, b; Eckhorn and Reitboeck 1988) in combination with signal correlation methods (e.g. Schneider et al. 1983; Gerstein and Aertsen 1985; Aertsen et al. 1986; Eckhorn et al. 1986; Melssen and Epping 1987; Palm et al. 1988; Eckhorn and Reitboeck 1988).

*What types of spatio-temporal signals might be involved in global coding?* Stimulus evoked oscillatory field potentials in the gamma range (30–110 Hz) were proposed to play a role in global sensory coding; Freeman and coworkers did extensive measurements on this topic in the rabbit olfactory bulb and cortex (e.g. Freeman and Skarda 1985). Oscillatory activities were found also in the cat and rat olfactory systems (Bressler and Freeman 1980), in a variety of structures of the cat brain (Başar 1983), in the cat primary visual cortex (Gray and Singer 1987a, b; Eckhorn et al. 1988a–c), and in the monkey visual cortex (Freeman and van Dijk 1987). In humans, SE-resonances were also found in EEG-recordings from the skull above association and motor areas (Krieger and Dillbeck 1987). Psychophysical experiments on eye movement reaction times indicate that internal periodic signals (30–40 Hz) play a role during visual perception and/or in the execution of oculomotor tasks (Pöppel and Logothetis 1986). Until recently, however, a direct relation between single cell tuning properties and the initiation of high frequency oscillatory activities has not been shown. Gray and Singer (1987a, b) were first to observe such dependency between the orientation of a moving stimulus and the initiation of oscillatory activities in cat primary visual cortex. The present investigation concentrates mainly on measurements of the spatial coherence distributions of stimulus-evoked resonances in the visual cortex. The results are interpreted in the context of a preliminary model for global visual coding. Some early results of this investigation were presented elsewhere (Eckhorn et al. 1988b, c).

## 2 Methods

### 2.1 Preparation

Adult cats were prepared semi-chronically. For the recordings initial anesthesia was induced by ketamine (Ketanest, 20 mg/kg, i.m.) and xylazine (Rompun, 2 mg/kg, i.m.) with a premedication of atropine (Atropin, 30 µg/kg, i.p.). During recordings, light anesthesia was maintained either with N<sub>2</sub>O/O<sub>2</sub> (70/30%), or ventilation with room air was used with small amounts of ketamine (1–2 mg/kg · h). If required, anesthesia was supplemented in both cases with halothane (Fluothan, 0.1–0.3%). Eye movements were blocked by infusion of alcuronium (Alloferin, 0.1 mg/kg · h). End-expiratory CO<sub>2</sub> (3.6%), body temperature (38°C), EEG and ECG were monitored continuously. The eyes were mydriated with atropine and neutral contact lenses with artificial pupils (3 mm diam.) were used in order to prevent the corneas from drying. The refraction was corrected with lenses to ensure a sharp retinal image of the stimuli projected onto a translucent screen 1.8 m in front of the cat.

### 2.2 Visual Stimulation and Recording of Neural Signals

Qualitative receptive field plots were obtained using a hand held projector. For quantitative analyses two independent computer-driven X-Y-mirror systems were available. A multi-electrode arrangement of 7 resp. 19 individually advanceable fiber-microelectrodes (250 or 330 µm apart; Reitboeck 1983a, b) was used to record from the primary visual cortex (A17 and A18). Interchangeable electrode guide heads with different electrode arrangements were available. From each electrode three different types of neural signals were separated in parallel: 1) Single-unit spikes (SUA) had to exceed an amplitude threshold (temporal accuracy: 0.1 ms). 2) From the compound signal, multiple-unit activities (MUA) were filtered with a bandwidth of 0.7–10 kHz; this signal was full-wave rectified and low-pass filtered in order to obtain the envelope (100 Hz cut-off frequency; 12 db/oct; sampled at 500/s. 3) Local field-potentials (LFPs) were filtered from the compound signal (13–250 Hz, in some cases 1–100 Hz; 12 db/oct; sampling rate 500/s).

### 2.3 Signal Analysis

Correlations between all combinations of the three signal types were calculated. For LFPs, normalized cross-correlation functions were obtained via the fourier domain over 250 ms response intervals (subtraction of the mean amplitude and multiplication by Blackman-Harris window prior to fourier transformation (Harris 1978); subsequent averaging in the frequency domain). Cross-event histograms were derived for SUA, and the correlations between SUA and

LFPs were obtained with spike-triggered averaging (STA). Estimates of the internally generated cooperative interactions between neurons were obtained by a simplified separation procedure in which correlations due to a common stimulus (the “shift predictor”) are subtracted from the “raw correlations” (improved estimation methods were recently developed and evaluated by Palm et al. 1988).

### 3 Results

#### 3.1 Stimulus Evoked Resonances in Local Assemblies

**3.1.1 Oscillatory Components in Different Types of Neural Signals.** Stimulus-evoked resonances (SE-resonances) were present in all of the three types of recorded neural signals; they were most obvious in LFPs where they could directly be seen on the oscilloscope in single sweeps (Fig. 1). Stimulus evoked rhythmic discharges of local neuron groups (MUA) were frequently weaker than those in LFPs. In single-unit spike trains (SUA) it is more difficult to detect the rhythmic component. Its presence was often evident, however, when the auto-coincidence histograms (Fig. 2, panels A3,4) or their amplitude spectra were computed (Fig. 2, panels B3,4).

**3.1.2 Stimulus Coupling of Evoked Oscillations.** Our preliminary results show that the occurrence of the oscillation spindles and their mean frequencies are stimulus dependent, but that the phases of the high frequency oscillations are not rigidly locked to stimulus phases. Stimulus-locked temporal averaging of LFP resonances, therefore, resulted in response histograms without oscillating components. The phases of the oscillatory components, hence, are determined by the neuronal network, and not by the stimulus. This is

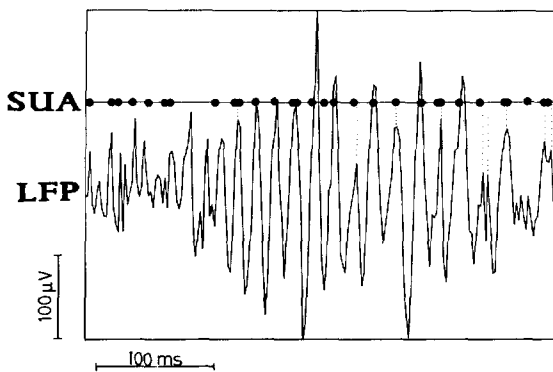


**Fig. 1.** Stimulus evoked oscillation. Single response epoch of a local field potential (LFP) and single-unit (SUA), recorded via the same electrode. *Stimulus:* grating, 0.7 cycles/deg drifted at 8 deg/s in preferred direction. LFP: negative polarity upwards. Note the transition from a stochastic to an oscillating state at about 100 ms. SUA: each dot denotes a spike

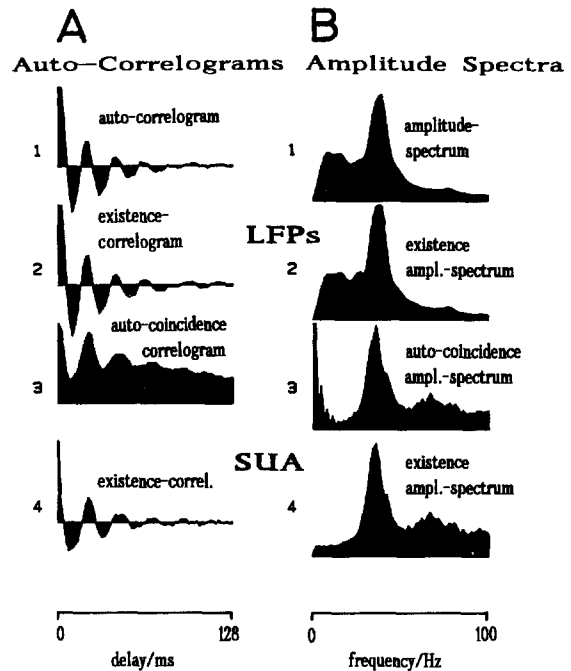


**Fig. 2A and B.** Signal properties of local field-potentials (LFPs) and single-unit spike activity (SUA) during the resonance state. Stimulation: as for Fig. 1. SUA and LFPs recorded via the same electrode. **A** Auto-correlograms of LFPs (1, 2), auto-coincidence histograms of SUA (3, 4); peak amplitudes at zero delay are clipped in the plots. **B** Amplitude spectra of the data in A. (Amplitude scaling: arbitrary, equal for 1–4)

shown in Fig. 2, where auto-correlograms and amplitude spectra of simultaneously recorded LFPs and SUAs are plotted together with their respective existence histograms. (For the calculation of existence functions see e.g., Melssen and Epping 1987). Note that the amplitudes of the oscillatory components in this example are not affected by subtraction of the stimulus-induced correlations (i.e. the phases of the oscillations are not stimulus dependent). Stimulus-response correlations, however, are strong with respect to the envelope of the neural signal. This can be seen in Fig. 3B where an orientation tuning curve is shown that was derived from post stimulus time histograms of LFP envelope signals.

**3.1.3 Oscillation Frequencies of SE-Resonances.** The spectral power density of SE-resonances had its maximum in the frequency range between 40 to 80 Hz (often at 40–50 Hz; Figs. 2B, 8, and 9B). This is in contrast to the more stochastic, broad-band frequency spectrum of the ongoing activities, where the spectral amplitude peaks appear at low frequencies (1–30 Hz; Fig. 9B, upper panels of the amplitude spectra). SE-resonance spindles had two distinct types of frequency variations: The “instantaneous frequency” often shifted to lower frequencies (e.g. in Fig. 1 from about

70 to 55 Hz; see also Gray and Skinner (1988): LFP-spindles of the rabbit's olfactory bulb). The second type of frequency variation is stochastic. Random variations are prominent when the dominating frequency components from responses to identical stimulus repetitions are compared (Fig. 8). The frequency of their peak amplitude can vary by 30 Hz and more. During ongoing neural activity, "spindles" of 30–60 Hz were also observed in LFPs. They occurred, however, less frequently and their amplitudes were less than half of those of the SE-resonances at the same recording position (preliminary qualitative results).

**3.1.4 Correlation Between LFP-Resonances and Single Unit Spikes.** Correlations between LFPs and SUA have been analyzed for the visual cortex (e.g. Creutzfeldt et al. 1966 (qualitative results); Gray and Singer 1987a, b) and for the rabbit's olfactory bulb (e.g. Freeman and Skarda 1985; Gray and Skinner 1988). We used the peak amplitude of the cross-correlation function between SUA and LFPs as a simple measure for the correlation strength. So far, we quantitatively studied more than 70 cells with respect to their involvement in local SE-resonances. In these cases SUAs and LFPs were recorded from the same electrode (see Fig. 6A). SUA-LFP correlation maxima up to 0.7 were found (peak of correlogram, normalized to spike rate and LFP amplitudes).

### 3.2 Stimulus Specificities of Oscillatory Signals

**"Receptive Fields" of SE-Resonances.** We determined the receptive fields (RFs) and "tuning properties of SE-resonances" for various stimulus parameters. RFs can be evaluated for SE-resonances by marking the area on the projection screen from which oscillatory responses can be elicited. Qualitative evaluations of such RFs were made with a hand held projector while the experimenters judged the amplitudes of the SE-resonances simultaneously on an oscilloscope and with a low frequency audio monitor. Several stimulus specificities were tested qualitatively: RF-position and -size, ocularity, orientation, direction and velocity of movement and ON/OFF-characteristics. These RF-properties were determined with SE-resonances of LFPs and MUA; they proved to be similar to those of local single cells, determined in the conventional way.

**Orientation/Direction Tuning of SE-Resonances.** The local orientation/direction tuning properties for SUA and LFP oscillations were found to closely resemble each other (Fig. 3). This means that SE-resonances of LFPs are associated with the primary coding properties (here: directional tuning) of single cortical neurons.

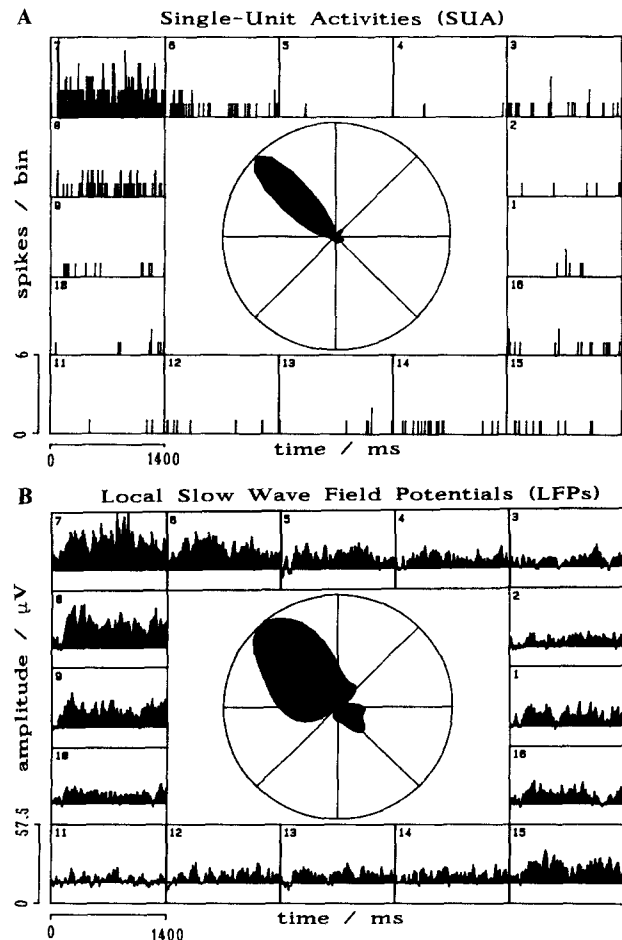


**Fig. 3A and B.** Orientation-/direction-tuning of local field potentials and single-unit spike activity recorded at the same cortical position. **A** SUA, **B** LFPs; both signals from the same electrode. Stimulus: as for Fig. 1. Frames: PSTHs (19 stimulus repetitions). Calculations for LFP-histograms: 1) subtraction of mean of total record, 2) rectification, 3) low-pass filtering by Blackman-Harris window ( $-3$  db at 100 Hz), 4) calculation of PSTH from single responses. Centers: Tuning for stimulus direction. Amplitudes were derived by integration over the histograms (mean spontaneous activity subtracted); amplitudes for intermediate directions were obtained by interpolation: 1) linear interpolation in cartesian coordinates, 2) low pass filtering by von-Hann window with a total width of 45 deg orientation

**Mean Frequency of SE-Resonances Depends on Stimulus Drift Velocity.** The type of visual stimulation was found to influence the frequency of the dominant spectral peak of oscillatory responses. Figure 4 shows 3 examples: The mean frequency of the spectral peak increased by about 5 Hz if the stimulus drift velocity was doubled. This logarithmic relation between drift velocity and frequency shift was found in A17 for a range of 1–20 deg/s and in A18 for 2–64 deg/s.

**SE-Resonance With Monocular Stimulation.** Binocular stimulation, in most cases, evoked

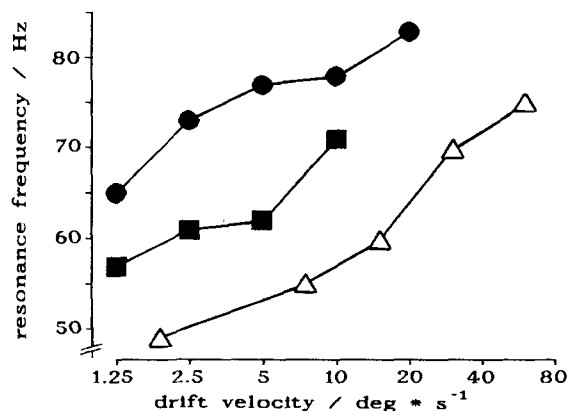


**Fig. 4.** Dependence of SE-resonance frequencies on stimulation. Here: dependence on movement velocity. Filled symbols: A17. Open symbols: A18. Stimulus: grating 0.7 cycles/deg; binocular stimulation; RFs of both eyes overlapped

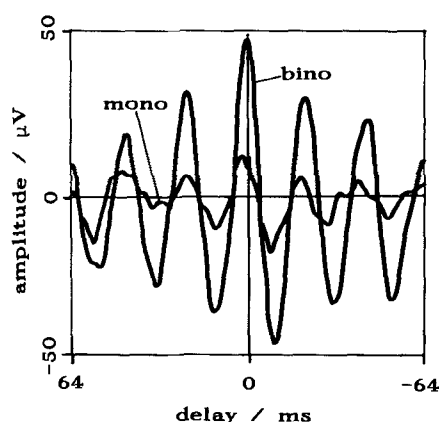


**Fig. 5.** Enhanced oscillation amplitudes with binocular compared to monocular stimulation. Here: Coherent oscillations in 2 different cortical areas. Correlation between spike train (A17, pos. 12 of Fig. 8) and LFPs (A18) calculated as spike-triggered LFP average. Stimulus: grating of 0.7 cycles/deg, drifting at 4 deg/s, optimally oriented with respect to the single-cell's RF. The A17 monocular RFs of the single cell overlapped with the A18 RFs. The RFs in A17 and A18 had the same ocularity. mono: monocular stimulation of dominant eye, bino: binocular; 100 trigger spikes for each correlogram

higher SE-resonance amplitudes than monocular stimulation of the dominant eye. Figure 5 shows an example where the correlation peak of the STA of LFPs was 3 times higher for binocular than for monocular stimulation. This is particularly interesting, since the binocular enhancement of the SE-resonances was observed as a coherent resonance phenomenon in two different visual areas: SUA was recorded in A17 and LFPs in A18 (see also chapter 3.3.2 and Fig. 7).

### 3.3 Coherence of SE-Resonances at Distant Cortical Positions

Coherence of SE-resonances was found 1) within a vertical cortex column, 2) between neighbouring hypercolumns, and 3) between two different cortical areas.

**3.3.1 Correlations Between SE-Resonances Within a Single Visual Area.** Phase-coupled SE-resonances were frequently found in signals recorded from neighbored electrodes of our arrays (250 resp. 330  $\mu\text{m}$  minimal distance) when the locally "preferred" stimulus was used. Within these electrode distances RF-properties of single units were often similar, except for one specific recording situation: in cross-orientation columns (Bauer and Fischer 1987; Eckhorn et al. 1988a) coherence of SE-resonances was found between the upper and lower layers although the orientation tunings of the single-units in these positions were orthogonal. Since SE-resonances are orientation/direction sensitive, it would be interesting to know whether upper or lower layer tuning dominates in generating the coherence.

We have been using *correlation profiles* (Fig. 6) to illustrate the spatial distributions of SE-resonance correlations. These were calculated with two methods: 1) spike-triggered averaging of LFPs (Figs. 6A and 7B), and 2) cross-correlation between LFPs (Fig. 6B). The correlation profiles were obtained by plotting the amplitude of the main peak in the normalized cross-correlograms versus cortical recording distance. A sequence of correlograms was calculated between a reference signal from one electrode and from each of the signals from the other electrodes of the linear array (Fig. 6; LFPs were band-pass filtered at 35–75 Hz). With the LFPs, e.g., on electrode 1 as a reference signal, the correlation peak decreases to a minimum of about 0.5 at a distance of 0.75 mm (electrode 4). At a distance of 1.25 mm the correlation strength increases and drops again at 1.5 mm. Subsequently, signals recorded by other electrodes were taken as reference in order to obtain the corresponding correlation profiles. Most profiles in Fig. 6B have a minimum at the center of the electrode array that might be related to functional properties of the underlying cortical matrix of hypercolumns (Hubel and Wiesel 1962). The shape of the correlation profiles in Fig. 6B indicates that cell groups with similar orientation/direction specificities are more strongly linked (electrodes 1, 2, 3, 6, 7) than neighbouring cell groups with different specificities (el. 4 and 5).

**Phase Relations of SE-Resonances.** SE-resonances recorded at distant cortical positions frequently had almost zero phase-lag. Zero-phase was found: 1) throughout all layers of the same *vertical cortex column*. This holds for both types, iso- and cross-orientation columns (for cross-orientation columns see Bauer and Fischer 1987), and 2) in tangential direction at sampling ranges within *adjoining columns*. At distances of 0.3–1.6 mm the coherence decreased by 50% ( $N=16$ ; measured within layers II/III). In tangential direction the coherence of the SE-resonances, usually, fell off without a significant phase shift.

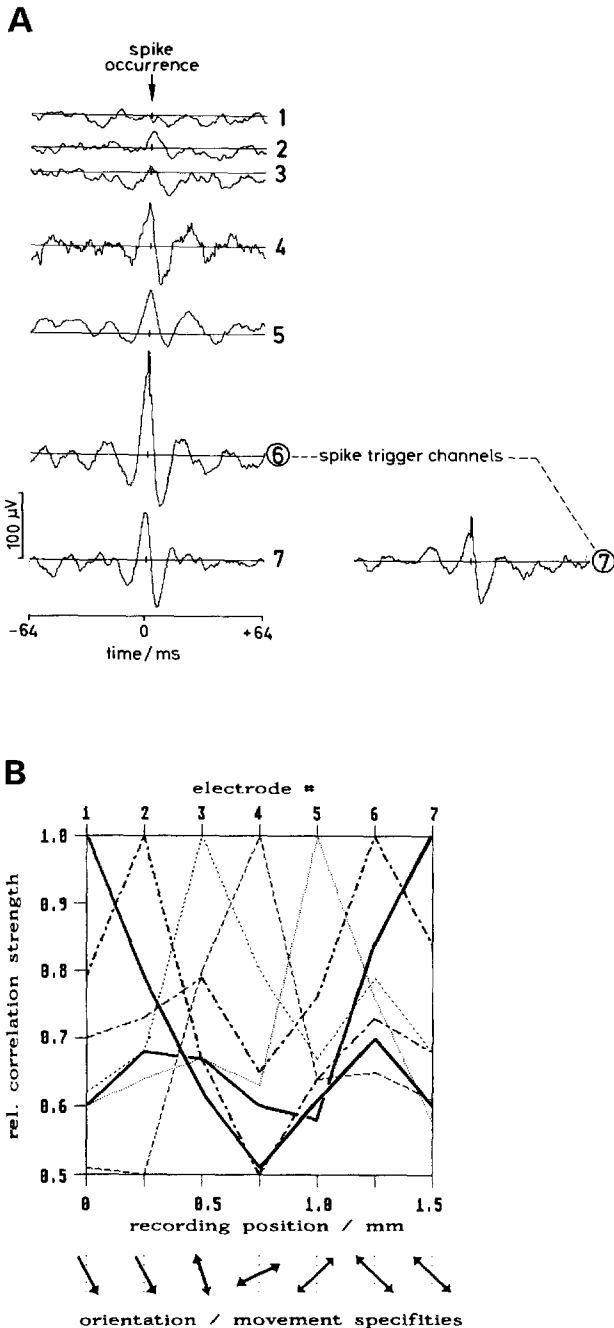


**Fig. 6A and B.** Horizontal extent of SE-resonance correlations within a single cortex area. **A** Simultaneous recordings of SUA and LFPs (layers II/III, A17). Cross-correlograms derived by STA of LFPs. Left: reference to spikes on electrode 6; right: reference spikes on electrode 7, normalized to the number of averages. Stimulus: grating 0.7 cys/deg drifting at 8 deg/s in and against preferred direction of single unit (el. 6). RFs of neighbouring recording positions overlapped. **B** Spatial correlation profiles of LFPs; recording by 7-electrode linear array in A17. The peak amplitudes of the normalized cross-correlograms are plotted over cortical distance. Each electrode was taken as reference for cross-correlations with the signals on the remaining electrodes. The orientation/direction specificities of single units at each recording position are indicated below. Same stimulus as for **A**, drifting in preferred direction of cells on electrodes 1, 2, 3 and 6, 7

**3.3.2 Coherence of SE-Resonances in Different Visual Cortex Areas.** Figure 7 shows an example for the spatial distribution of the coherence of SE-resonances in the two visual areas (A17 and A18). We scanned A17 along recording tracks down the medial bank of the central sulcus over about 2.5 mm, while the activity in A18 was recorded with two stationary electrodes. Along the tracks, SUA was recorded at multiple positions in A17. SUA-LFP correlations were calculated using spike-triggered averaging. Highly correlated SE-resonances were found at two “columnar recording positions” in A17 (about 1.2 mm apart) in which the orientation preferences were similar to those of the A18 position. At electrode positions 1 and 2 the single units’ RFs had, however, no overlap with the A18 fields and their directional preference was in the opposite direction, while in the second “resonance patch” (position 7 and 12) the RFs

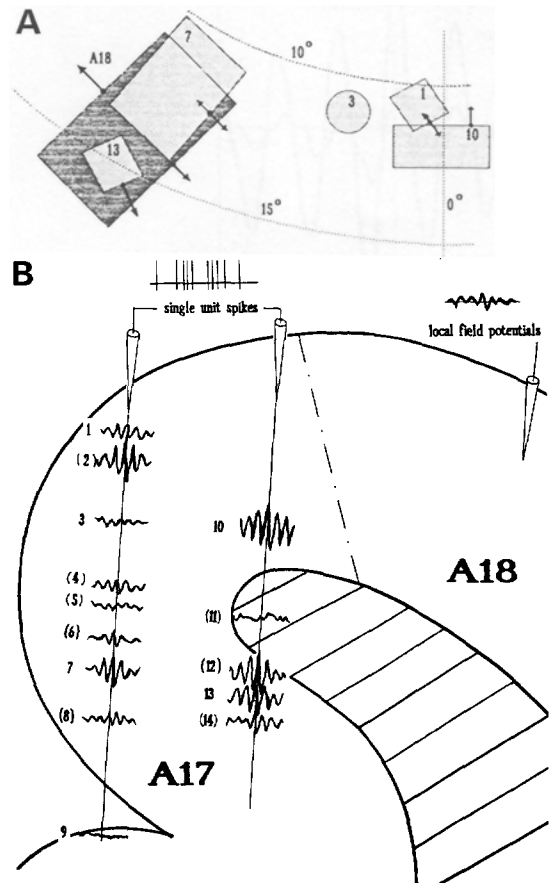


**Fig. 7A and B.** Coherent oscillations in visual areas A17 and A18. Recordings of LFPs in A18 at a fixed position and of SUA at successive positions in two electrode tracks in A17. Signal-correlations between the 2 cortical areas were derived by STA of LFPs. **B** In spike recording positions the respective STA-correlograms are plotted (frontal section at posterior P2, left hemisphere). **A** Relative RF-positions and -areas; numbers denote recording positions, arrows the directionality of the cells. Stimulus: binocular, grating 0.7 cys/deg drifting in preferred direction at 8 deg/s

overlapped and these cells preferred a movement direction opposite to that in A18.

The coherence of LFPs in A17 and A18 was also measured in experimental situations as shown in

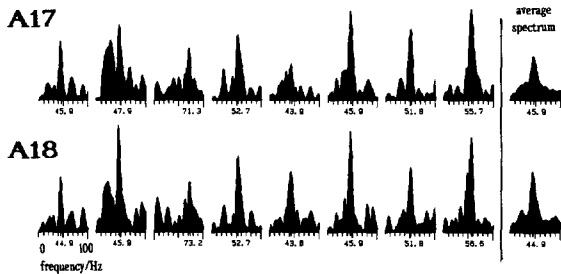


**Fig. 8.** Coherent oscillations in 2 visual cortical areas (A17 and A18). Short-epoch (250 ms) amplitude frequency spectra of LFPs. Spectra of responses to the same stimulus interval (grating of 0.7 cycles/deg drifting at 8 deg/s). Left panel: single epoch spectra. Right panel: average of 19 single epoch spectra. Note 1) the wide frequency range of the peak amplitudes in single epoch spectra, 2) similarities of peak frequencies in A17 and A18

Fig. 7. In order to estimate frequency variations and phase locking of SE-resonances in both areas we calculated the amplitude spectra of LFPs, recorded at corresponding positions in the visual representation (position 7 of Fig. 7). The left panels of Fig. 8 show spectra of single 250 ms responses, recorded within the same interval of the stimulus cycle. The narrow spectral peaks are distributed over a relatively wide range (44–73 Hz). These frequency variations were identical in signals from both areas (resolution limit: about 1.9 Hz).

*Time Course of Correlated LFPs in two Visual Areas.* Figure 9 shows the time course of stimulus-evoked coherent oscillations of LFPs at two corresponding positions of the visual representations in A17 and A18. Binocular stimulation with a whole field grating evoked large amplitude oscillations of about 45 Hz (Fig. 9A). After the stimulus stopped moving, the activity became more stochastic, with broad-band frequency components (Fig. 9B and C). The maxima of

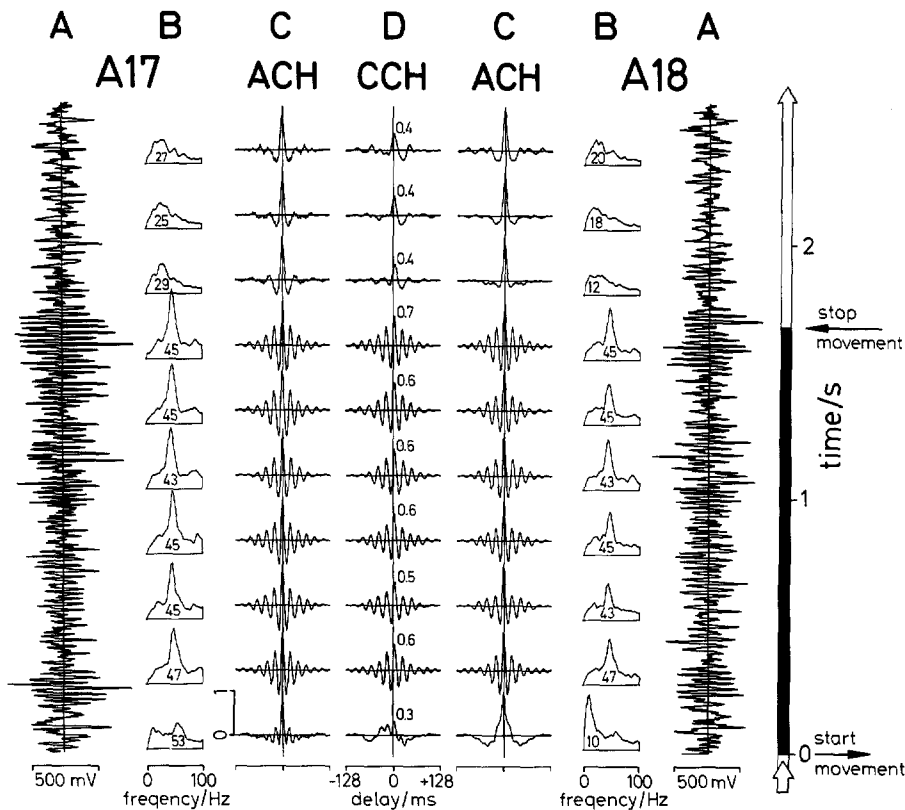


**Fig. 9.** Time course of coherent oscillations at corresponding positions in 2 different visual cortex areas. Local field potential recordings from primary visual areas A17 and A18 of the cat (position 6 of Fig. 8). Recording bandwidth ( $-3$  db), A17: 13–250 Hz, A18: 1–100 Hz. Binocular stimulation with grating (0.7 cycles/deg) swept at optimal direction with 8 deg/s (“optimal” for local single-unit spike responses). Black bar and arrows denote the period of stimulus movement. Left: data from A17; Right: data from A18. A: Single sweep LFP recordings. Note the oscillatory activation during stimulus movement and the transition to a more stochastic state after stimulus stop. B: Amplitudes of the LFP frequency spectra, calculated for successive 256 ms epochs; averaging in the frequency domain of 19 responses. Note the peak at about 44 Hz appearing at start of stimulus movement and disappearing at stop. Numbers in the spectrograms denote the frequency of the maximum. C: Autocorrelation functions, calculated by FFT transformation from the data of B. Note the stimulus evoked oscillations. D: Normalized cross-correlation functions calculated from the respective 256 ms LFP epochs. Numbers at the correlation peaks denote their amplitudes

the short-period (250 ms) normalized correlograms were taken as a measure for the overall correlation strength between the LFPs of both areas. Correlation was relatively high during the entire stimulus period, changing from about 0.4 during stationary presentation to about 0.6 during stimulus movement. The shape of the cross-correlograms reveals, however, that different types of signal components determine the correlograms derived under moving and stationary stimulation (Fig. 9D).

## 4 Discussion

### 4.1 Coherence of SE-Resonances at Distant Cortical Positions

We consider the appearance of coherent SE-resonances at functionally close but spatially distant locations of the visual cortex to be the most important result of this investigation. SE-resonances were found to be phase-locked throughout all layers of a vertical column. Coherent oscillations were also generated between neighbouring columns, and they were even found in different cortical areas when the local oscillators had some common primary coding properties. These observations are essential prerequisites of our model of global visual coding. In this model, correlated activity is assumed to act as a label to link related features in a visual scene and to signalize the momentary association. Our finding that coherent SE-resonances appear in remote cortical regions differs from the experimental observations of Gray and Singer (1987a, b). They found independent activity patterns limited to the dimensions of a single orientation column. Differences in experimental techniques are possible reasons for these different results.

*Phase-Coupling Between SE-Resonances in Distant Cortical Positions.* The frequencies of the SE-resonances were temporally unstable during a spindle and they varied also in response to identical stimuli (Fig. 8). Coherence, therefore, is obviously not induced by direct frequency control via the stimulus but rather by a neural phase locking mechanism. What could be the underlying mechanism that near-zero phase lag appears between signals from spatially distant structures?

Othmer (1984) modelled various types of neural coupling with respect to their influence on synchronization and phase-locking. A variety of interneuronal connections can lead to coherent oscillations: 1) Bottom-up entrainment by a common driver with (one-way or, better, mutual) excitatory connections, 2) Top-down entrainment from a higher cortical area by a "supervisor circuit" (one or two way; see Grossberg 1976, 1980), 3) Mutual excitatory connections at the same level of organization (either within a cortical area or between parallel areas). If an extra-

cortical "entraining structure" exists, its oscillations should be coherent with cortical ones. Up to now this has not been shown for SE-resonances in the visual system.

Freeman and coworkers extensively investigated oscillatory phenomena in EEG-recordings of the rabbit olfactory system. They developed a computer model of the olfactory system, indicating that the crucial parameter for state changes in their network (from stochastic to oscillating behaviour) is *mutually excitatory feedback gain* among neurons (Freeman and Skarda 1985). It seems plausible that a network with similar properties might also be responsible for the coherent oscillations in cat visual cortex. Such phase-locking mechanisms probably are not realized via additive interactions, because these would influence the primary coding properties by forming larger RFs, i.e. the spatial resolution of the system would deteriorate. Non-linear interactions, such as multiplications or Boolean AND-operations would be more appropriate for mediating phase-locking.

*Anatomical evidence* that excitatory connections play a primary role in the cortex is well documented in the literature. Clustered excitatory connections extending horizontally over several millimeters were identified within the primary visual cortex (e.g. Gilbert and Wiesel 1983). Massive reciprocal connections among different cortical areas were found to be distributed in isolated patches. Generally, these connections are considered to be mutually excitatory and to terminate at correspondent positions of the visual representation (e.g. Symonds and Rosenquist 1984).

*Physiological evidence* for excitatory intracortical connections has been reported for the cat primary visual cortex. Using cross-correlation techniques Ts'o and coworkers found that distribution and range of the excitatory interactions do correspond to the clustering and extent of the horizontal connections observed anatomically (Ts'o et al. 1986). They stated, that "the extent of the horizontal connections and their facilitatory nature suggests that they may contribute to properties beyond those determined by classical receptive field analyses". However, they did not propose functional roles for the long range excitatory connections. These axons have small diameters and low conduction velocities (about 1 m/s). Connected assemblies that simultaneously exhibit SE-resonances, could, therefore, be phase-locked within half an oscillation cycle up to distances of 10 mm at 50 Hz.

### 4.2 Coherent SE-Resonances in Different Visual Areas

If our results are confirmed, two important facts can be stated for the cooperation of A17 and A18: 1) Coherent SE-resonances between LFPs of A17 and A18 can extend over a range of at least 2 hypercolumns. 2)

Patches of neurons in A17 can generate action potentials that are correlated with SE-resonances of LFPs in A18. In previous experiments we found “correlation patches” in A17 and A18 (defined by the maxima in the coupling between their ongoing MUAs (Eckhorn et al. 1988a; Reitboeck et al. 1987)). In some instances we could prove that the correlation patches overlapped with those positions from which orthodromic trans-synaptic stimulation elicited action potentials, and that functionally coupled structures appeared at those positions that were retrogradely labelled in A17 after a HRP-injection in A18 (Eckhorn et al. 1988a). Since all of these anatomical and functional patch structures are separated by about 1 mm, it can be assumed that they are related to the functional units of the visual cortex, the hypercolumns (Hubel and Wiesel 1962). Up to now we could not confirm whether the correlated A17/18-activities (ongoing and/or SE-resonances) are due to a common external subcortical or cortical input, whether they are due to the massive reciprocal A17/18 feedback loops that had been demonstrated anatomically or whether they are due to a combination of both. This question is presently studied in some of our ongoing experiments.

*Role of the A17/18 Connections.* We propose that the main function of the reciprocal excitatory connections between A17 and A18 is to establish phase-locking between assemblies that represent the linking features of the actual visual scene. No other plausible functional role has been claimed so far for the massive reciprocal connections between A17 and A18 in the cat. Functional elimination of either A17 or A18 in the cat by cooling or ablation of one of the areas did not basically alter the primary coding properties of single units in the intact area (e.g. Donaldson and Nash 1975; Sherk 1978).

#### 4.3 Stimulus Dependency of Local SE-Resonances

*Receptive Fields of SE-Resonances.* The restricted spatial extent of the receptive fields of SE-resonances of LFPs indicates that these signals are obviously not mediated by extracellular “far field” volume conduction. This finding is also supported by the fact, that RFs for LFP oscillations, determined for two recording positions in A17 with about 1.2 mm separation, clearly did not overlap. SE-resonances of LFPs are, probably, mainly due to a superposition of the local excitatory dendritic potentials. This follows from the same arguments as given by Mitzdorf (1987) for the interpretation of cortical current source density distributions.

#### 4.4 Stimulus-Evoked Coherent Oscillations and Global Coding

We propose that the coherence of SE-resonances at distant cortical positions as observed in our experiments are likely to constitute a second “higher” stage of

sensory coding. The coherent oscillations would be well suited to define global aspects of a visual scene by linking related features. Elementary features are assumed to be evaluated in the primary coding stages, i.e. they are defined by the RF-properties of single cortical and subcortical neurons. The proposed second step in visual coding is global and it is, therefore, basically different from RF-coding. *The phase-coupling* between local assemblies during their oscillatory state is a suitable mechanism to serve the following purposes: 1) SE-resonances are linking excitatorily connected neurons with similar RF-properties. By this means transient dynamic assemblies can define local regions based on such parameters as homogeneity of visual features and/or simultaneous activation. 2) SE-resonances are transiently pacing the input to and output from a vertical cortical column. 3) Spatially distant but functionally closely connected assemblies that transiently represent linking features are labelled for their similarity, continuity and simultaneity by coherent oscillations. We are convinced that SE-resonances are a general phenomenon, forming the basis of a correlation code which is used within and between different sensory systems and perhaps even throughout the entire brain.

*Acknowledgements.* We are grateful to our colleagues, especially to Drs. F. Gonzalez, F. Krause, J. Leferink, and J. I. Nelson. Many thanks to W. Gerber, W. Lenz, P. Muth, U. Thomas, and J. H. Wagner for their expert help in experimental techniques. We are thankful to Drs. A. Aertsen and G. Curio for improving the manuscript and for many helpful suggestions. (Supported by DFG grants Re 547/2 and Ba 636/4).

#### References

- Aertsen A, Gerstein G, Johannesma P (1986) From neuron to assembly: neuronal organization and stimulus representation. In: Palm G, Aertsen A (eds) Brain theory. Springer, Berlin Heidelberg New York, pp 7–24
- Altmann L, Eckhorn R, Singer W (1986) Temporal integration in the visual system: influence of temporal dispersion on figure-ground discrimination. *Vision Res* 26:1949–1957
- Başar E (1983) Synergetics of neural populations. A survey on experiments. In: Başar E, Flohr H, Haken H, Mandell AJ (eds) Synergetics of the brain. Springer, Berlin Heidelberg New York, pp 183–200
- Bauer R, Fischer WH (1987) Continuity or discontinuity of orientation columns in visual cortex: a critical evaluation of published and unpublished data. *Neuroscience* 22:841–847
- Bressler SL, Freeman WJ (1980) Frequency analysis of olfactory system EEG in cat, rabbit and rat. *Electroencephalogr Clin Neurophysiol* 5:19–24
- Creutzfeldt OD, Watanabe S, Lux HD (1966) Relation between EEG-phenomena and potentials of single cells. *Electroencephalogr Clin Neurophysiol* 20:1–37
- Donaldson IML, Nash JRG (1975) The effect of a chronic lesion in cortical area 17 on the visual responses of units in area 18 of the cat. *J Physiol* 245:325–332
- Eckhorn R, Reitboeck HJ (1988) Assessment of cooperative firing in groups of neurons. In: Başar E (ed) Springer Series in Brain

- Dynamics, vol 1. Springer, Berlin Heidelberg New York, pp 219–227
- Eckhorn R, Schneider J, Keidel R (1986) Real-time covariance computer for cell assemblies is based on neuronal principles. *J Neurosci Methods* 18:371–383
- Eckhorn R, Bauer R, Reitboeck HJ (1988a) Discontinuities in visual cortex and possible functional implications. In: Başar E, Bullock TH (eds) Dynamics of sensory and cognitive processing by the brain. Springer Series in Brain Dynamics, vol 2. Springer, Berlin Heidelberg New York, pp (in press)
- Eckhorn R, Bauer R, Brosch M, Jordan W, Kruse W, Munk M (1988b) Functionally related modules of cat visual cortex show stimulus-evoked coherent oscillations: A multiple electrode study. *Invest Ophthalmol Vis Sci* 29:331, 12
- Eckhorn R, Bauer R, Brosch M, Jordan W, Kruse W, Munk M, Reitboeck HJ (1988c) Are form- and motion-aspects linked in visual cortex by stimulus-evoked resonances? Workshop: “Visual Processing of Form and Motion”, European Brain & Behavior Society, Tübingen (Confer abstr vol P7)
- Freeman W, van Dijk BW (1987) Spatial patterns of visual cortical fast EEG during conditioned reflex in a rhesus monkey. *Brain Res* 422:267–276
- Freeman WJ, Skarda CA (1985) Spatial EEG patterns, non-linear dynamics and perception: the Neo-sherringtonian view. *Brain Res Rev* 10:147–175
- Gerstein G, Aertsen A (1985) Representation of cooperative firing activity among simultaneously recorded neurons. *J Neurophysiol* 54:1513–1528
- Gilbert CD, Wiesel TN (1983) Clustered intrinsic connections in cat visual cortex. *J Neurosci* 3:1116–1133
- Gray CM, Singer W (1987a) Stimulus specific neuronal oscillations in the cat visual cortex: a cortical functional unit. *Soc Neurosci (abstr)* 404.3
- Gray CM, Singer W (1987b) Stimulus-dependent neuronal oscillations in the cat visual cortex area 17. *Neuroscience [Suppl]* 22:1301P
- Gray CM, Skinner (1988) Centrifugal regulation of neuronal activity in the olfactory bulb of the waking rabbit as revealed by reversible cryogenic blockade. *Exp Brain Res* 69:378–386
- Grossberg S (1976) Adaptive pattern classification and universal recoding: II, Feedback, expectation, olfaction, illusions. *Biol Cybern* 23:187–202
- Grossberg S (1980) How does a brain build a cognitive code? *Psych Rev* 87:1–51
- Harris FJ (1978) On the use of windows for harmonic analysis with the discrete fourier transform. *Proc IEEE* 66:51–83
- Hubel DH, Wiesel TN (1962) Receptive fields, binocular interaction, and functional architecture in the cat's visual cortex. *J Physiol* 160:106–154
- Johannesma P, Aertsen A, van den Boogaard H, Eggermont J, Epping W (1986) From synchrony to harmony: ideas on the function of neural assemblies and on the interpretation of neural synchrony. In: Palm G, Aertsen A (ed) Brain theory. Springer, Berlin Heidelberg New York, pp 25–47
- Koenderink J (1984) The concept of local sign. In: van Doorn AJ, van de Grind WA, Koenderink J (eds) Limits in perception. VNU Sci Press, Utrecht, pp 495–549
- Krieger D, Dillbeck M (1987) High frequency scalp potentials evoked by a reaction time task. *Electroencephalogr Clin Neurophysiol* 67:222–230
- Melssen WJ, Epping WJM (1987) Detection and estimation of neural connectivity based on crosscorrelation analysis. *Biol Cybern* 57:403–414
- Mitzdorf U (1987) Properties of the evoked potential generators: current source-density analysis of visually evoked potentials in the cat cortex. *Intern J Neurosci* 33:33–59
- Othmer HG (1984) Synchronization, Phase-locking and other phenomena in coupled cells. In: Rensing L, Jaeger NI (eds) Temporal order. Springer, Berlin Heidelberg New York, pp 130–143
- Palm G, Aertsen AMHJ, Gerstein GL (1988) On the significance of correlations among neuronal spike trains. *Biol Cybern* 59:1–11
- Pöppel E, Logothetis N (1986) Neuronal oscillations in the human brain. *Naturwissenschaften* 73:2667–2670
- Reichardt W (1957) Autokorrelations-Auswertung als Funktionsprinzip des Zentralnervensystems (bei der optischen Wahrnehmung eines Insektes). *Z Naturforsch* 12b:448–457
- Reichardt W, Poggio T, Hausen K (1983) Figure-ground discrimination by relative movement in the visual system of the fly. Part II: Towards the neural circuitry. *Biol Cybern* 46 [Suppl]:1–30
- Reitboeck HJ (1983a) A 19-channel matrix drive with individually controllable fiber microelectrodes for neurophysiological applications. *IEEE SMC* 13:676–682
- Reitboeck HJ (1983b) A multi-electrode matrix for studies of temporal signal correlations within neural assemblies. In: Başar E, Flohr H, Haken H, Mandell AJ (eds) Synergetics of the brain. Springer, Berlin Heidelberg New York, pp 174–182
- Reitboeck HJ (1988) Neural mechanisms of pattern recognition. In: Lund J (ed) Sensory processing in the mammalian brain: neural substrates and experimental strategies. Oxford University Press, New York, pp 420–465
- Reitboeck HJ, Eckhorn R, Pabst M (1987) A model of figure/ground separation based on correlated neural activity in the visual system. In: Haken H (ed) Synergetics of the brain. Springer, Berlin Heidelberg New York, pp 44–54
- Reitboeck HJ, Pabst M, Eckhorn R (1988) Texture description in the time domain. In: Cotterill MJ (ed) Computer simulation in brain science. Cambridge University Press, Cambridge (in press)
- Schneider J, Eckhorn R, Reitboeck HJ (1983) Evaluation of neuronal coupling dynamics. *Biol Cybern* 46:129–134
- Sherk H (1978) Area 18 cell responses in cat during reversible inactivation of area 17. *J Neurophysiol* 41:204–215
- Symonds LL, Rosenquist AC (1984) Corticocortical connections among visual areas in the cat. *J Comp Neurol* 229:1–38
- Ts'o D, Gilbert CD, Wiesel T (1986) Relationships between horizontal interactions and functional architecture in cat striate cortex as revealed by cross-correlation analysis. *J Neurosci* 6:1160–1170
- Von der Malsburg C (1983) How are nervous structures organized? In: Basar E, Flohr H, Haken H, Mandell AJ (eds) Synergetics of the brain. Springer, Berlin Heidelberg New York, pp 238–249
- Von der Malsburg C, Schneider W (1986) A neural cocktail-party processor. *Biol Cybern* 54:29–40
- Wilson JTL, Singer W (1981) Simultaneous visual events show a long-range spatial interaction. *Percept Psychophys* 30:107–113

Received: July 4, 1988

Prof. Dr. R. Eckhorn  
 Fachbereich Physik  
 Angewandte Physik und Biophysik  
 Philipps-Universität  
 Renthof 7  
 D-3550 Marburg  
 Federal Republic of Germany